Full-size field test of prestressed concrete T-beam bridge

Ensink, Sebastiaan; van der Veen, Cor; Hordijk, Dick; Lantsoght, Eva; van der Ham, Herbert; de Boer, A.

Publication date
2018

Document Version
Accepted author manuscript

Published in
Structural Faults & Repair 2018 and European Bridge Conference 2018

FULL-SIZE FIELD TEST OF PRESTRESSED CONCRETE T-BEAM BRIDGE

S.W.H Ensink &
C. van der Veen &
D.A. Hordijk
Delft University of Technology
Faculty of Civil Engineering
& Geosciences
Stevinweg 1, 2628 CN Delft
The Netherlands

E.O.L. Lantsoght
Politécnico,
Universidad San
Francisco de Quito,
Diego de Robles y
Pampite, Sector
Cumbaya, EC170157
Quito, Ecuador

H. van der Ham
Ministry of
Infrastructure and
the Environment
Griffioenlaan 2,
3526 LA Utrecht
The Netherlands

A. de Boer
Consultant,
Arnhem,
The Netherlands

KEYWORDS: collapse test; experiment; prestressed concrete; bridge girder; beam; shear.

ABSTRACT
In the Netherlands, approximately 150 prestressed T-beam bridges with cast-in-between decks and mainly built in the sixties are still in service. Upon assessment, the prestressed beams often do not fulfil the design codes requirements, whereas upon inspection, they show no signs of distress. For the assessment, additional load transfer mechanisms, which could significantly enhance their structural capacity, such as compressive membrane action and transverse redistribution, are not considered. The presented research aims at quantifying these effects. Therefore, an existing simply supported multi-span T-beam bridge was tested. In total seven experiments were carried out using a single point load placed on the T-beam. Three experiments were carried out with the original structural system unchanged. In four experiments, the cast-in-between deck was sawn in longitudinal direction, so that the individual behaviour of the beams could be tested. In both cases two load positions, i.e. a distance of 2.25 m and 4.00 m from the support were used. By analysing both the single beam and the connected beam tests a better understanding of the load carrying capacity of this type of bridge is achieved.

INTRODUCTION

A large number of the existing bridges in the Netherlands were built in the 60's and 70's. Upon assessment, engineers are confronted with the fact that the live loads currently prescribed by NEN-EN 1991-2+C1:2015 are heavier than prescribed by the previous national codes, and that the shear capacity from the current provisions in NEN-EN 1992-1-1+C2:2011 is lower than in the previous national codes. A large number of existing bridges are thus analytically found to be insufficient for shear.

One subset of the Dutch bridge stock (150 bridges) that is shear-critical consists of prestressed T-beam bridges with cast-in-between decks. Load-carrying mechanism that are not considered for assessment include the effect of compressive membrane action in the deck (transverse direction), arch action in the beam (longitudinal direction) or transverse load (re)distribution from the analysed beam to the adjacent beams at the ultimate limit state.

Experimental data that quantify the transverse load distribution for shear in prestressed T-beam bridges with cast-in-between decks is limited to results from diagnostic load tests, or the distribution factors are based on linear finite element analyses. For beam bridges, the test data are limited to slab-beam bridges, for which the deck is cast on top of the beams instead of in between the beams (Arockiasamy and Amer 1998, Jáuregui and Barr 2004, Wekezer et al. 2004, Mordak and Manko 2008, Idriss and Liang 2010). Additional difficulties for the assessment of the existing prestressed T-beam bridges with cast-in-between decks in the Netherlands are the very low shear reinforcement ratios, the presence of cross-beams (Cai et al. 2002), and the presence of transverse prestressing.

DESCRIPTION OF VECHT BRIDGE

Location, structural system, and geometry

One typical example of an existing prestressed T-beam concrete bridge with cast-in-between decks is the Vecht Bridge near the town of Muiden in the province of Noord Holland in the Netherlands. This bridge was built in 1962, and consists of nine simply supported spans of which one is a movable bridge over the Vecht river. For each driving direction, a parallel bridge was built. The bridge was situated in the A1 highway. This highway is now rerouted, so that it became possible to test the bridge prior to its demolition. A partial overview of the bridge structure is given in Figure 1, showing the western approach ramp. Figure 1 also marks the investigated spans and the location of the cross-beams highlighted in span 2. The experiments on the connected beams were carried out on span 4, whereas the experiments on the individual beams were carried out on span 2. For the material investigations span 3 was used.

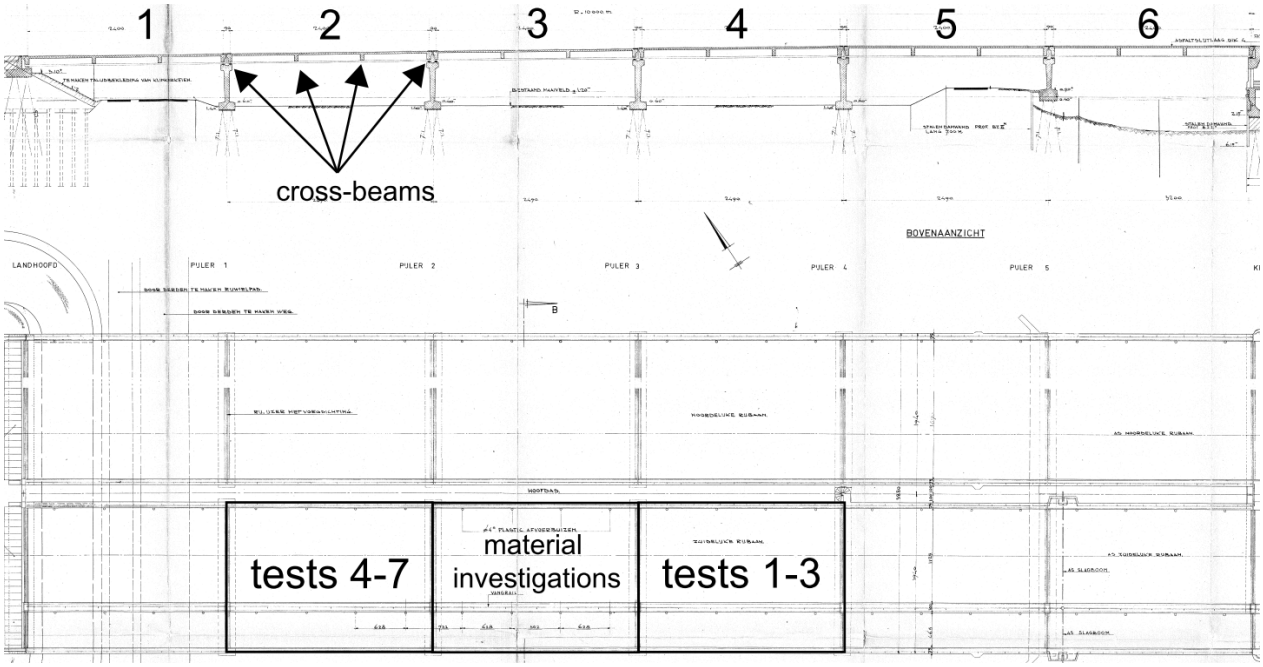

Figure 1 Partial overview of Vecht Bridge, longitudinal section (top), top view (bottom).

All spans are simply supported and 24 m long, and consist of 15 identical prestressed beams with cross-beams at 8 m intervals (i.e. 4 per span, see Figure 1). An overview of the bridge deck cross-section is given in Figure 2. The center-to-center distance between the beams is 1225 mm. Figure 2 also shows the cast-in-between slab which is only connected to the T-beams by transverse prestressing.

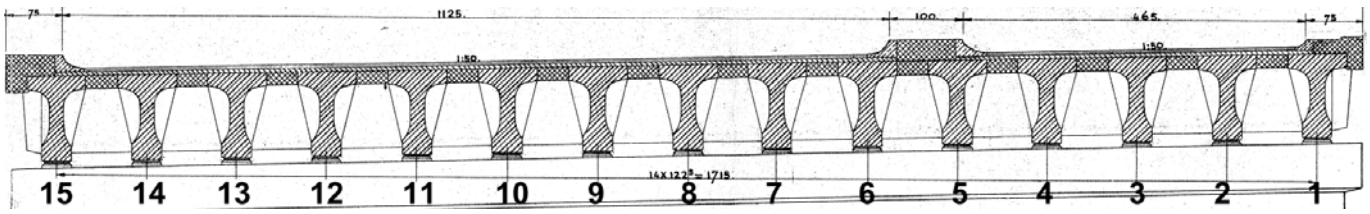

Figure 2 Cross-section of Vecht Bridge (measurements in cm).

The details of the beams are given in Figure 3. The thickness of the cast-in-between deck is equal to the height of the top flange of 180 mm. The beam has a 750 mm long end block with a thickness equal to the bottom flange (i.e. 400 mm), and a 1000 mm long transition piece between the end block and the ‘standard’ cross section. In Figure 3 (right) the ducts of the transverse prestressing in the top flange, i.e. at

the center of the cast-in-between slab, and at the location of the cross-beam are shown. In total the transverse prestressing consist of 59 tendons per span. In longitudinal direction, the T-beam is prestressed with seven curved prestressing tendons of which six are anchored at the end block and one is anchored in the deck. Note that the beams were prefabricated on-site and pretensioned after which all the ducts were grouted.

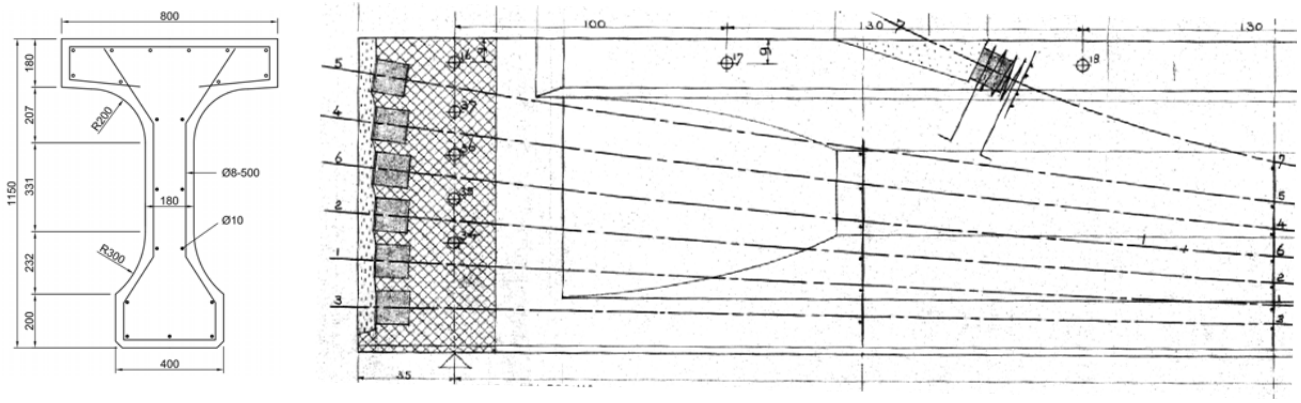

Figure 3 Cross section beam with reinforcement, measurements in mm (left), side view of beam close to the support showing the curved prestressing cables, measurements in cm (right).

Material properties concrete, prestressing and reinforcement

Both the longitudinal as well as the transverse prestressing consist of tendons with 12ø7 mm strands (A_p = 462 mm^2). Prestressing steel qualities QP150 and QP170 were used during the era of construction of the Vecht Bridge. In the laboratory, the measured properties were f_y = 1505 MPa for the yield strength and f_u = 1770 MPa for the ultimate tensile strength (Koekkoek 2017), which corresponds to steel quality QP170. The transverse prestressing results in an average concrete compressive stress in the deck of approximately 4 MPa.

The longitudinal steel reinforcement in the T-beams consists of 5ø10 mm in the bottom flange, and 10ø10 mm bars in the top flange. In the web, 6ø10 mm bars are present, see Figure 3 left. The shear reinforcement (stirrups) consists of only ø8-500 mm. Note that this amount of shear reinforcement is much less than the minimal value prescribed by NEN-EN 1992-1-1+C2:2011: $\rho_w = 0.112\ \% << \rho_{w,min} = 0.215\ \%$. It is also noteworthy that the shape of the stirrup follows the shape of the T-beam, i.e. is not straight, which is also not in accordance with the detailing requirements for stirrups in NEN-EN 1992-1-1+C2:2011. The mild steel quality is QR24 with a measured yield strength in the laboratory of f_y = 288 MPa and an ultimate tensile strength of f_u = 352 MPa. As mentioned before note that, with the exception of the transverse prestressing, there is no steel reinforcement connecting the cast in-between slab to the beam.

The average concrete cube compressive strength $f_{ck,cube}$ on the original drawings is 50 MPa. However, on span 3 (see Figure 1) an extensive investigation into the material properties of the concrete has taken place (den Boef 2016, Remans and Kerk 2016). The average concrete compressive strength was found to be: $f_{cm,cube}$ = 107.6 MPa (web of the beams), $f_{cm,cube}$ = 101.5 MPa (bottom flange of the beams), $f_{cm,cube}$ = 111.1 MPa (top flange of the beams), and $f_{cm,cube}$ = 73.5 MPa (cast-in-between deck). In addition, a relatively large aggregate size (D_{max}) was observed from the drilled cylinders in excess of 50 mm.

TEST SETUP

Load positions and test preparations

In total seven experiments were carried out. The numbering of the experiments can be found in Figure 1 and Table 1. The numbering of the beams is shown in Figure 2. Prior to the experiments, the asphalt was first removed by an asphalt ripper in such a way as to minimize damage to the concrete deck. In span 2, the cast-in-between deck was sawn in longitudinal direction, so that the individual behaviour of the beams could be tested. Additionally, three of the four cross-beams, with the exception of the end cross-beam opposite to the load location, are sawn, see Figure 4. This was done as to prevent uncontrolled rotation during the single beams tests.

Figure 4 Sawing through the cast-in-between slab (left), sawing and drilling through the cross-beams (right).

In span 4, the original structural system was not changed. In test 1 and 2 at least four beams are present between the tested beam and the edge of the bridge. Therefore, in these tests a significant load distribution to the adjacent beams will take place. In test 3 the edge beam itself was tested. The load position 'a' at 4000 mm (center support to center load position) is chosen because of its position midway between the cross-beams. The load position at 2250 mm is chosen as the weakest cross-section for an individual beam due to the position of the prestressing tendon anchored in the top flange (see Figure 3 right). Note, that the effective depth 'd' used in Table 1 is variable: at a = 4000 mm, d = 835 mm, and at a = 2250 mm, d = 720 mm.

Table 1 Overview of tests.

test	span	*a* (mm)	a/d	beam number	structural system	type of test
1	4	4000	4.8	11	not changed	Intermediate beam
2	4	2250	3.1	6	not changed	Intermediate beam
3	4	2250	3.1	1	not changed	Edge beam
4	2	2250	3.1	12	sawn	Individual beam
5	2	2250	3.1	11	sawn	Individual beam
6	2	2250	3.1	10	sawn	Individual beam
7	2	4000	4.8	9	sawn	Individual beam

Loading system

The full loading system consists of a 25 m steel spreader beam with ballast on top. The span of the steel spreader just exceeds the span of the concrete bridge, with the supports for the steel spreader located on the adjacent spans. The load is applied as a single concentrated load of 400 × 400 mm placed on the T-beam by using a hydraulic jack. When the hydraulic jack extents and presses against the steel spreader, the load can be gradually applied from the steel spreader beam to the concrete bridge. In the first three

tests, additional ballast was used near the support at the opposite side, as to prevent uplifting of the steel spreader. Additionally, a sliding system was provided to easily change from one test location to the next. The full system is shown in Figure 5. Before sliding to the next test location some of the ballast was temporarily removed.

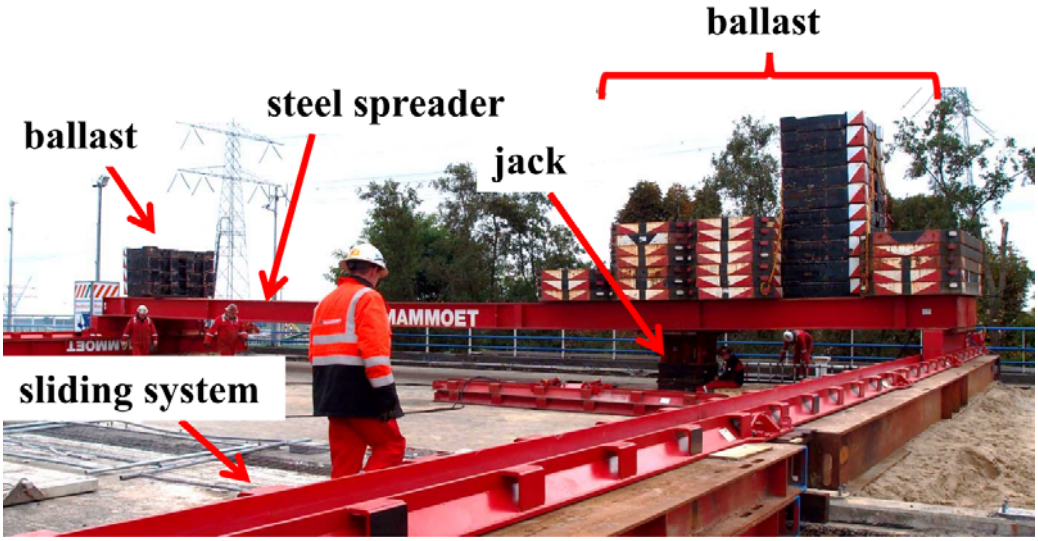

Figure 5 Test setup loading system.

For the individual beams in span 2 a safety system was put in place to prevent a complete collapse of a beam. This was achieved by steel chains around the beams for which holes were drilled through the deck. The chains are anchored in place by a steel beam placed in transverse direction, so that the tested beam would be caught by the chains in the event of a complete collapse of the beam, see Figure 6.

Figure 6 Safety system for single beam tests (steel chains), top side (left), bottom side (right).

Applied measurements

The measurements that were applied during the experiments determined the applied force at the jack, the vertical deformations of the loaded beam, the adjacent beams as well as the elastomeric bearings at the supports, and the longitudinal strain at the bottom flange of the beam, see also Figure 7. The force was measured with a load cell, and all displacements were measured with LVDTs. The longitudinal strain under the point load was measured by applying an LVDT horizontally over 1 m. Therefore, it could be observed during the experiment when the cracking moment of the tested beam was reached, see Figure 7 (right). Additionally, on both sides of the tested beam camera's where placed to continuously take photos and record video. Finally, a radar interferometry system was used during the first two experiments, to evaluate if in future field tests, the contact measurements can be replaced by non-contact measurements. For more details about the measurement the reader is referred to (Koekkoek 2017).

Figure 7 Vertical LVDT at support (left), horizontal LVDT at bottom flange beam (right)

TEST RESULTS

Experiments on span 4 (connected beams)

In span 4, three experiments were carried out in order to investigate the behaviour of the beams within the structural system. Therefore, a single point load of 400 x 400 mm was placed directly on the T-beam. The test setup for test 1 is also shown in Figure 5. Both test 1 and 2 resulted in a shear failure of the loaded beam, see Figures 8 and 10. However, in both cases the shear failure of the beam is preceded by a punching failure of the loading plate through the top flange of the beam and the slab, see Figure 9. Of course, at the instant the punching failure occurs the load distribution to the adjacent beams is largely lost and the loaded beam suddenly receives the full loading resulting in an immediate shear failure. The punching failure was somewhat unexpected and could have been prevented by using a larger loading plate or multiple point loads.

Figure 8 Shear failure beam test 1

Figure 9 Punching failure deck test 1


Figure 10 Shear failure beam test 2

The load-displacement graphs for tests 1 and 2 are shown in Figures 11 and 12. In these tests the displacement of the adjacent beams, at the same distance from the support, was also measured. It was observed that, in both tests 1 and 2 a large shear crack occurred from the loading position in the opposite

direction towards the first intermediate cross-beam, see Figure 10 (left). Especially for test 2 this was somewhat unexpected since the distance from the load to the support was 2250 mm, whereas the distance from the load to the intermediate cross beam was 5750 mm. As shown in Figure 11 and 12, for test 1 and 2 the failure loads are 3004 kN and 3444 kN respectively. However, it can be argued that the ultimate failure load in both tests would have been higher if the punching failure could have been prevented. Also the load was applied as a single point load whereas normally the live load would consist of a number of axel loads as well as distributed loads.

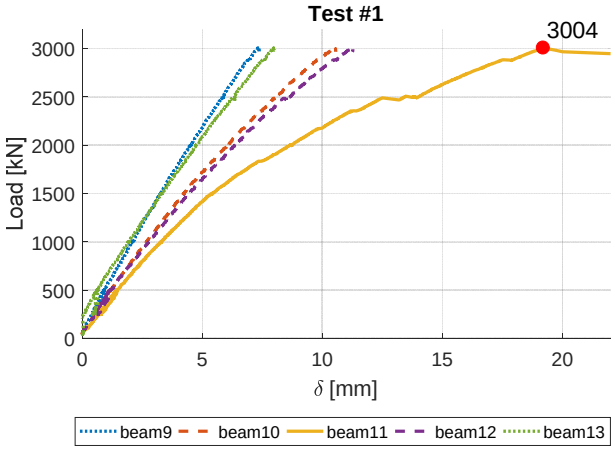

Figure 11 Load-displacement beam test 1.

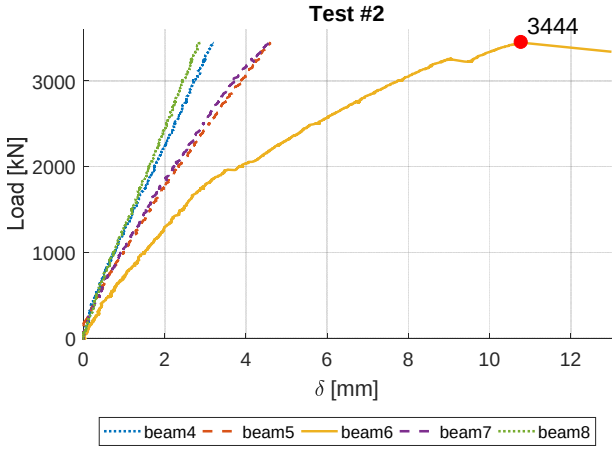

Figure 12 Load-displacement beam test 2.

Test 3 was carried out on an edge beam. Because of the stability of the test setup, it was decided not to load the beam past 2500 kN. At this load level, no failure occurred, and after unloading no major cracking was observed in the edge beam.

Experiments on span 2 (single beams)

In span 2, four experiments were carried out on individual beams. Tests 4-6, with the load at a distance from the support of a = 2250 mm, all resulted in a shear failure of the beam at respectively 1634 kN, 1703 kN and 1774 kN, see Figures 13, 14 and 15. Test 7, with the load at a distance from the support of a = 4000 mm, resulted in a shear failure at 1022 kN, see Figure 16.

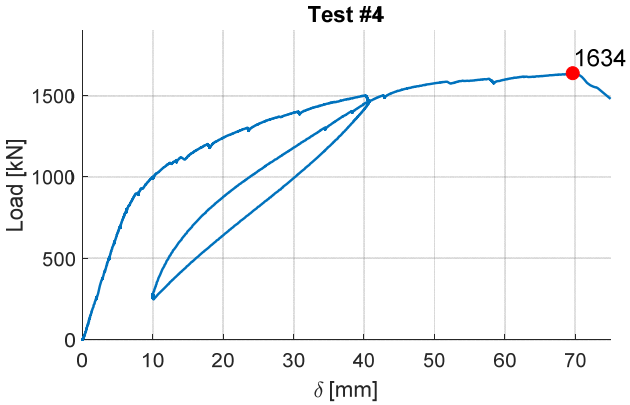

Figure 13 Load-displacement beam test 4

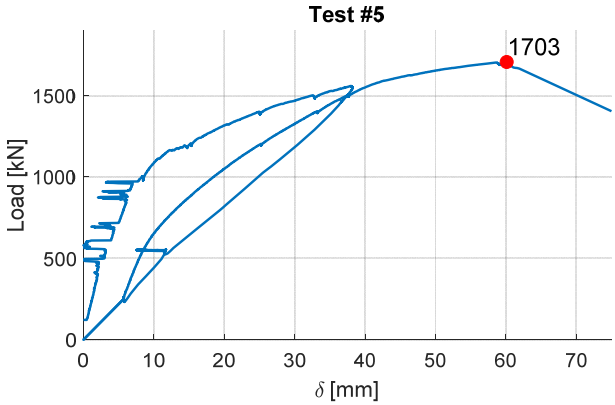

Figure 14 Load-displacement beam test 5

Halfway during test 4 and 5 as well as during test 7, unloading was necessary to be able to adjust the safety chains as shown in Figure 6, in order to accommodate the observed deformations of the beam. The shear failure itself can be seen in Figures 17 and 18. In test 7 the beam almost completely separated into two parts being kept together only by the prestressing tendons.

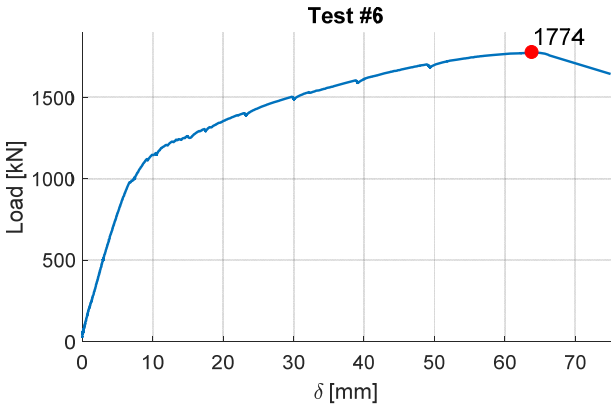

Figure 15 Load-displacement beam test 6

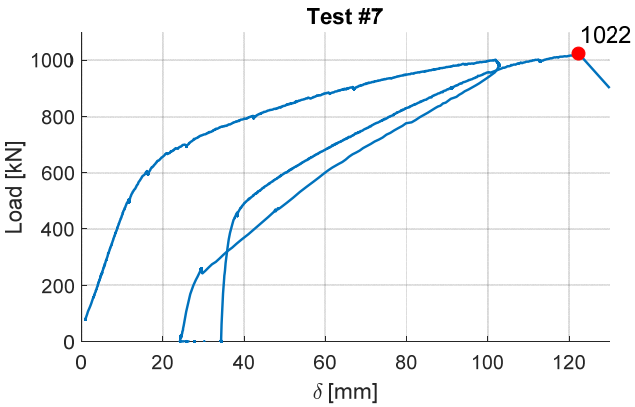

Figure 16 Load-displacement test 7

Figure 17 Shear failure beam test 4 and 5

Figure 18 Shear failure beam test 6 and 7

CROSS SECTIONAL ANALYSIS

Introduction

In this section the experimental results are compared with cross-sectional checking for shear and bending, using average values, according to Eurocode 2 (NEN-EN 1992-1-1+C2:2011). For prestressed beams the following failure modes are considered: shear bending (SB), shear tension (ST), ultimate bending moment (M_u) and bending cracking moment (M_{crack}). Note that shear tension is only valid in parts of the beam that are uncracked by bending. In these parts, the bending cracking moment itself is considered to be the limit value for shear tension resistance. Also note that for shear bending, due to the lack of sufficient stirrups, only the concrete resistance is taken into account. Finally, for shear tension, the maximum principal stress is calculated and checked over the full height of the beam.

Connected beam tests 1 and 2

For the cross-sectional checking of test 1 and 2 the load distribution is first calculated using a linear elastic finite element model. The finite element model consists of a plate model with eccentric ribs. The plate part represents the cast-in-between slab as well as the top flange of the prestressed beams. The remaining part of the prestressed beams and the cross beams are modelled using eccentric ribs. An overview of this model is given in Figure 19. The loading only consists of the point load placed at the center of a beam at the locations used in the experiments. The next step is to evaluate the internal forces, shear (V), bending moment (M), and normal force (N) of the loaded beam at every 200 mm interval. The prestressing forces and the dead weight are calculated separately at the same locations. Now for every value of the external load (F) the combined internal forces, i.e. external load + dead weight + prestressing,

at every 200 mm interval can be determined. As an example, for test 1 the bending and shear forces are given in Figures 20 and 21 using a unity load of F = 1000 kN (a = 4000 mm). Due to the geometry of the curved prestressing tendons (Figure 3) and the presence of the end block, the internal forces arising from the prestressing are somewhat irregular. From Figures 20 and 21 it becomes clear that the intermediate cross beam (at x = 8 m) plays an important role in the load distribution.

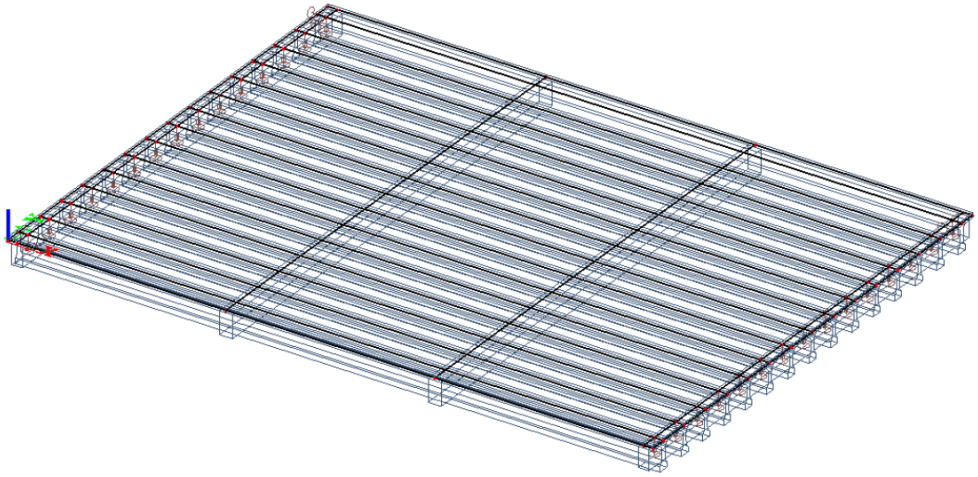

Figure 19 Linear elastic finite element model, plate with eccentric ribs.

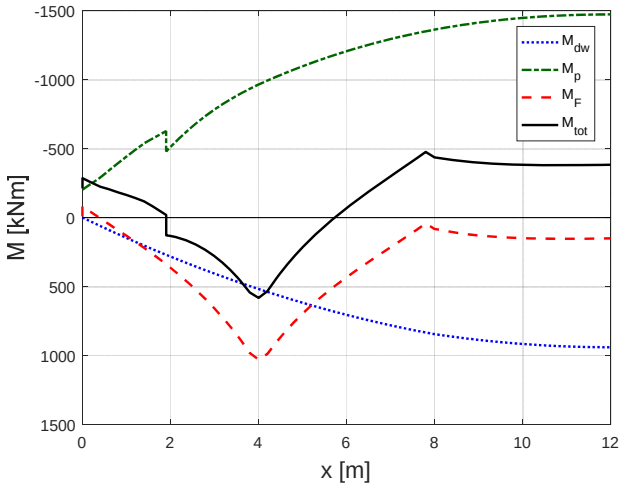

Figure 20 Bending moment, Dead weight (dw), Prestressing (p), external load (F) and total (tot).

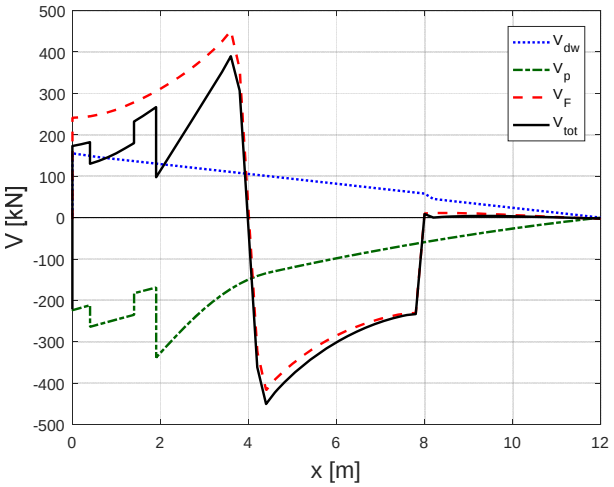

Figure 21 Shear forces, Dead Weight (dw), Prestressing (p), external load and total (tot).

For the cross-sectional checking a Matlab routine is used. The Matlab routine evaluates all cross-sections automatically. For each cross-section and for each failure mode, the external force (F), is multiplied in such a way that a unity check of 1.00 is achieved. In this way, the maximum load for each cross-section and for each failure mode is determined. The results of the cross-sectional checking for test 1 and 2 using the Matlab routine are given in Figures 22 and 23. For test 1, the maximum load F_{max} is calculated as 1580 kN, and the failure mode is shear tension (ST). Compared to the experimental failure load of 3004 kN, there is a huge discrepancy with the analytically found resistance. For test 2, the maximum load F_{max} is calculated as 1753 kN, and the failure mode is again shear tension (ST). Again compared to the experimental failure load of 3444 kN, there is a huge discrepancy with the analytically found resistance. Due to the fact that the bending cracking moment is considered to be the limit value for shear tension resistance, the resistance value with the load at a = 2250 mm is found to be somewhat higher than at a = 4000 mm.

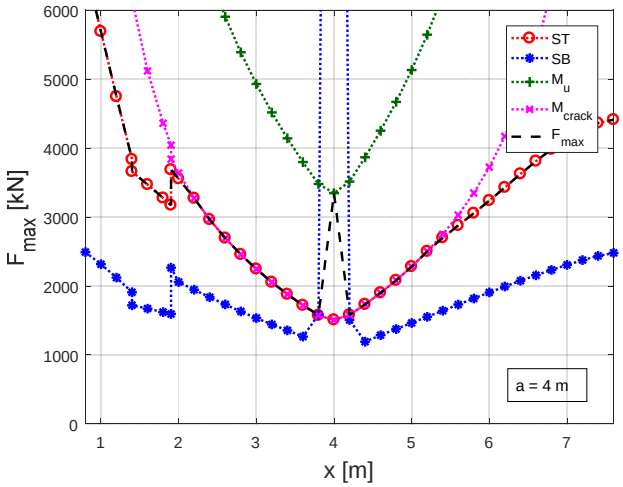

Figure 22 Cross-sectional checking test 1

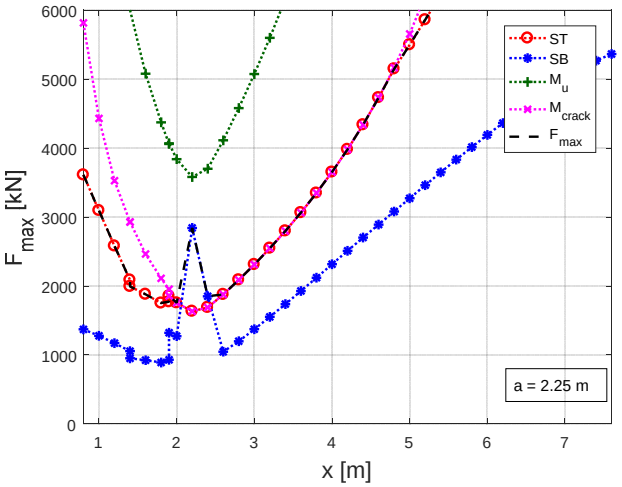

Figure 23 Cross-sectional checking test 2

Single beam tests 4-7

For the single beam tests, the internal forces can be readily calculated without the use of a finite element model. In the calculation the opposite end of the beam is assumed to be fully clamped due to the presence of the untouched cross-beam. The same procedure as with the connected beams is applied to perform the cross-sectional checking using the Matlab routine. The results of the cross-sectional checking for tests 4-6 and 7 using the Matlab routine are given in Figures 24 and 25. For tests 4-6, the maximum load F_{max} is calculated as 733 kN, and the failure mode is shear bending (SB), whereas the average value in the experiments was 1704 kN. Also, it seems the failure load in the experiments is slightly larger than the maximum load calculated for the ultimate bending moment of 1600 kN. A possible explanation is that the prestressing forces are somewhat underestimated (to calculate the prestressing forces, 20% of time dependent losses are taken into account). In test 4-6 it seems that the shear resistance is underestimated by a factor of 2.3. For test 7, the maximum load F_{max} is calculated as 751 kN, and the failure mode is again shear bending (SB), whereas in the experiment a failure load of 1022 kN was found.

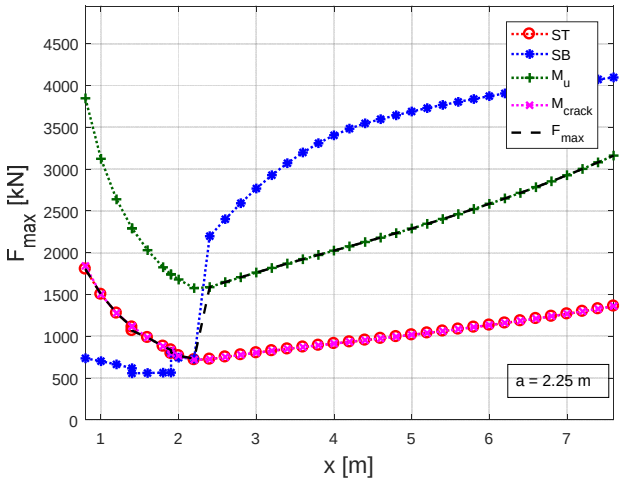

Figure 24 Cross-sectional checking tests 4-6

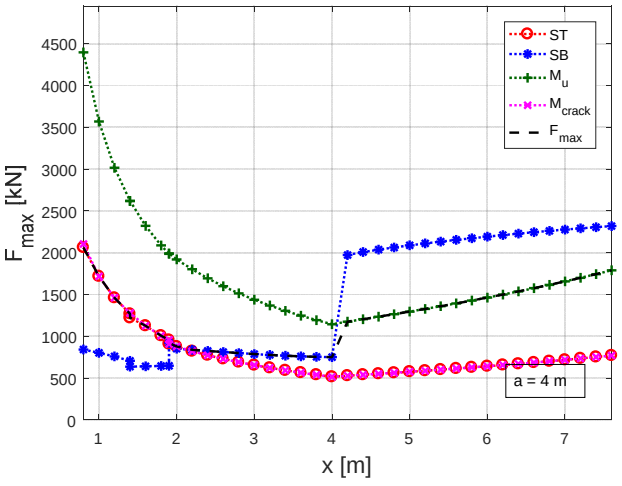

Figure 25 Cross-sectional checking test 7

SUMMARY AND CONCLUSIONS

To extend the knowledge of existing concrete bridges, and of prestressed T-beam bridges with cast-in-between slab and transverse prestressing in particular, seven large full-size field tests are executed. The experiments show that very high loading can be resisted by the bridge deck in case of the connected beam tests. In these tests in fact, the loading with an individual point load was even higher than the combined

force of three lanes of heavy truck loads according to Eurocode. Also, it can be argued that the ultimate failure load in both tests would have been even higher if the punching failure could have been prevented. When comparing the experimental results of test 1 and 2 with the cross-sectional checking according to Eurocode 2, large discrepancies are found with the experimental load being almost a factor of two higher than the analytically found resistance when using average values. This emphasizes the need to further investigate the mechanism that could possibly explain these large discrepancies. When comparing the individual beam tests with the cross-sectional checking the experimental loads are also much higher than the analytically found resistance. This is especially the case for tests 4-6 where it is observed that the shear tension resistance is much higher.

ACKNOWLEDGEMENTS

The authors wish to express their gratitude and sincere appreciation to the Dutch Ministry of Infrastructure and the Environment (Rijkswaterstaat) for financing this research work. The contributions and help of our colleagues Rutger Koekkoek, Marco Roosen, Fred Schilperoort and Yuguang Yang, and of student Thomas Harrewijn of Delft University of Technology are gratefully acknowledged. The fruitful discussions with Sonja Fennis from the Dutch Ministry of Infrastructure and the Environment, with Frank Linthorst and Danny den Boef of Witteveen+Bos, responsible for logistics and safety during the test, and with the late Chris Huissen and Otto Illing of Mammoet, responsible for applying the load during the pilot proof load tests, are also acknowledged.

REFERENCES

AROCKIASAMY, M. & AMER, A. 1998. Load Distribution on Highway Bridges Based On Field Test Data: Phase III.

CAI, C. S., SHAHAWY, M. & PETERMAN, R. J. 2002. Effect of Diaphragms on Load Distribution of Prestressed Concrete Bridges. *Transportation Research Record,* 1814**,** 47-54.

DEN BOEF, D. 2016. Proof loading bridge "Vecht Bridge A1" - Material research concrete compressive strength (in Dutch). Deventer, the Netherlands.

IDRISS, R. L. & LIANG, Z. 2010. In-Service Shear and Moment Girder Distribution Factors in Simple-Span Prestressed Concrete Girder Bridge - Measured with Built-in Optical Fiber Sensor System. *Transportation Research Record,* 2172**,** 142-150.

JÁUREGUI, D. V. & BARR, P. J. 2004. Nondestructive Evaluation of the I-40 Bridge over the Rio Grande River. *Journal of Performance of Constructed Facilities,* 18**,** 195-204.

KOEKKOEK, R. T. 2017. Measurement Report Loading of Vechtbrug (25H-100). Stevin Report 25.05-17-03. Delft University of Technology, Delft, the Netherlands.

MORDAK, A. G. & MANKO, Z. 2008. Static Load Tests of Posttensioned, Prestressed Concrete Road Bridge over Reservoir Water Plant. *Transportation Research Record,* 2050**,** 90-97.

REMANS, D. & KERK, L. K. 2016. Results concrete compressive strength (in Dutch). TNO.

WEKEZER, J., KWASNIEWSKI, L. & MALACHOWSKI, J. 2004. Analytical and experimental evaluation of existing Florida DOT bridges.